J. Cent. South Univ. (2015) 22: 2014−2019
DOI: 10.1007/s11771-015-2723-3

Springer

Microstructure characteristics and effect of grain orientation on magnetic properties of $Fe_{63}Co_{32}Gd_5$ alloy ribbons

YAO Wen-jing(姚文静)[1, 2], WANG Nan(王楠)[1], LEE Je-hyun[2]

1. Key Laboratory of Space Applied Physics and Chemistry of Ministry of Education (School of Science, Northwestern Polytechnical University), Xi'an 710129, China;
2. Engineering Research Center for Integrated Mechatronics Materials and Components, Changwon National University, Changwon 641−773, Korea

Abstract: By using the melt spinning techniques, the $Fe_{63}Co_{32}Gd_5$ alloy ribbons with 15−50 m in thickness and 3−7 mm in width were prepared at the wheel speeds of 15, 20, 25 and 35 m/s. The rapid solidification microstructures were characterized by three layers, the middle layer of which reaches 80% thickness and forms the column grain of (Fe,Co) solid with Gd solution. Grain refinement takes place with the increase of the wheel speed. And after 0.5 h heat treatment at 823 K, the ribbon thickness becomes larger and the middle layer of column grain is very orderly perpendicular to the ribbon plane. The coercivity of quenched and annealed $Fe_{63}Co_{32}Gd_5$ ribbons both have the inflection point at the wheel speed of 20 m/s, and the tendency is declining. The heat treatment processing makes the coercivity become lower by improving the order of $(Fe,Co)_{17}Gd_2$ compound. The saturation magnetization of quenched ribbons increases with the enhancement of wheel speed, whereas that of annealed ones decreases firstly and then increases. The minimum coercivity is 5.30×10^3 A/m and the maximum saturation magnetization is 163.62 $A\cdot m^2/kg$, which is obtained in the conditions of the wheel speed of 35 m/s and 0.5 h heat treatment at the temperature of 823 K.

Key words: Fe-Co-Gd alloy ribbon; rapid solidification; phase composition; magnetic properties

1 Introduction

Intermetallic compounds involving the rare earth and transition metals, especially 3D elements, have taken much research interests due to their excellent magnetic properties. Especially, the alloys containing the rare earth (RE) metal Gd and ferromagnetic transition metals (TM) Fe, Co and Ni are prospective candidates for potential magnetocaloric applications and are investigated extensively [1−6]. Addition of Gd will improve the physical and mechanical properties of many alloys, e.g., when small amount of Gd metal is added to Fe-based alloys, it will enhance the heat resistance and life-span of the alloys. For the new magneto-optical storage technology, Gd-Fe-Co magneto-optical materials have great potential applications. The investigation of Gd-Fe-Co alloy on the relationship between the microstructures and the magnetic properties is paid much attention to.

The melt spinning technique is succeeded in preparing alloy ribbons with the excellent magnetic properties, such as Nb-Fe-Co-V-B, Ni-Mn-Co-Sn, and Sm-Co-Fe-Cu-Zr-B [7−12]. For such a method, the grain orientation and grain size have interactive contributions as the wheel speed increases. On one hand, the high wheel speed makes the grains prefer to grow perpendicular to the ribbon plane due to the anisotropic external heat flux and the well orientated grains will form [13], and thus may increase the permeability. On the other hand, the decrease of the grain size with the wheel speed will increase the coercive force. In fact, this technique is one method to provide high cooling rate and considerable nucleation, which leads to a significant decrease of the grain size. Moreover, under the melt-spinning conditions, the average size of the phase inside the grain also decreases drastically. This is very different from the case in the casting ingots. Refined grain size should have contribution to improving the magnetic properties. Because the melt spinning process involves these two effects in one single process for obtaining ideal magnetic materials ribbons with specific performances, the interactive effect of the grain orientation and grain size should be examined.

In the present work, the $Fe_{63}Co_{32}Gd_5$ alloy was prepared by the melt spinning techniques at different

Foundation item: Projects(51271149, 50901060) supported by the National Natural Science Foundation of China; Project(NPU-310201401007JCY01007) supported by the Nothwestern Polytechnical University (NPU) Foundations for Fundamental Research, China; Project(2012-0009451) supported by the National Research Foundation of Korea
Received date: 2014−05−13; **Accepted date:** 2014−10−11
Corresponding author: LEE Je-hyun, Professor, PhD; Tel: +82−55−213−3695; E-mail: ljh@changwon.ac.kr

wheel speeds. The different magnetic properties of the quenched and annealed ribbons are measured for a comparison. The effect of the wheel speed on the rapid solidification microstructures and then on the magnetism characteristics are studied. The influence of grain orientation on the magnetic properties is discussed with the relation to the variation of wheel speed.

2 Experimental procedures

$Fe_{63}Co_{32}Gd_5$ master alloys were prepared from pure Fe (99.8%), Co (99.99%) and Gd (99.9%) by induction melting technique. The mass of each sample is about 5 g. The wheel diameter in the melt spinning technique is 110 mm and four wheel surface velocities were used: 10, 15, 20 and 35 m/s. During experiments, the samples were placed into a ϕ 12 (inner diameter)×ϕ 15 (outer diameter)×200 mm quartz tube with a ϕ 0.5 mm orifice at the bottom and were overheated to about 100 K above the melting point. Then, Ar gas flew into the tube and was blown the melt onto the rotating wheel surface through the orifice, producing spun ribbons. A following heat treatment was performed to show the annealing effect: ribbons were annealed at temperature of 823 K for 30 min in an Ar atmosphere flow environment, and then cooled in the furnace to the room temperature. The microstructures of the ribbons were observed by the optical microscopy, FEI Sirion 200 SEM and INCA Energy 300 EDS. The constitute phases were examined by the Cu K_α X-ray diffraction. The saturation magnetization was measured by the LakeShore 735VSM vibrating sample magnetometer.

3 Results and discussions

3.1 Microstructures and phase composition

By using the current experimental conditions, the ribbons 15−50 m in thickness and 3−7 mm in width were produced. They are flexible remarkably and their solidification microstructures are shown in Fig. 1. Normally, the ribbons show layered structures at the wheel velocities of 15, 20, 25, and 35 m/s. In Fig. 1(a), the obvious four layers form in ribbon. Near the free surface and the roller surface, the layer of single phase locates as wall. Between two walls, the equiaxed grain occupies the lower layer, and the dendrite grains are in the upper one. Figure 1(b) displays that the column grain appears in the middle layer of ribbons. Some free nucleation happens in the ribbon of 25 m/s, as presented in Fig. 1(c). With the increase of the wheel speed, the thickness of surface layers increases, and the layers of equiaxed grain and column grain become stronger. Figure 1(d) shows the rapid solidification microstructures of quenched ribbon at 35 m/s wheel speed, the thickness of which is almost a half of the ribbon at 20 m/s.

After the heat preservation of 30 min at 823 K, the microstructure of ribbon displays three clear layers, as shown in Fig. 2. The thickness of surface layer is larger

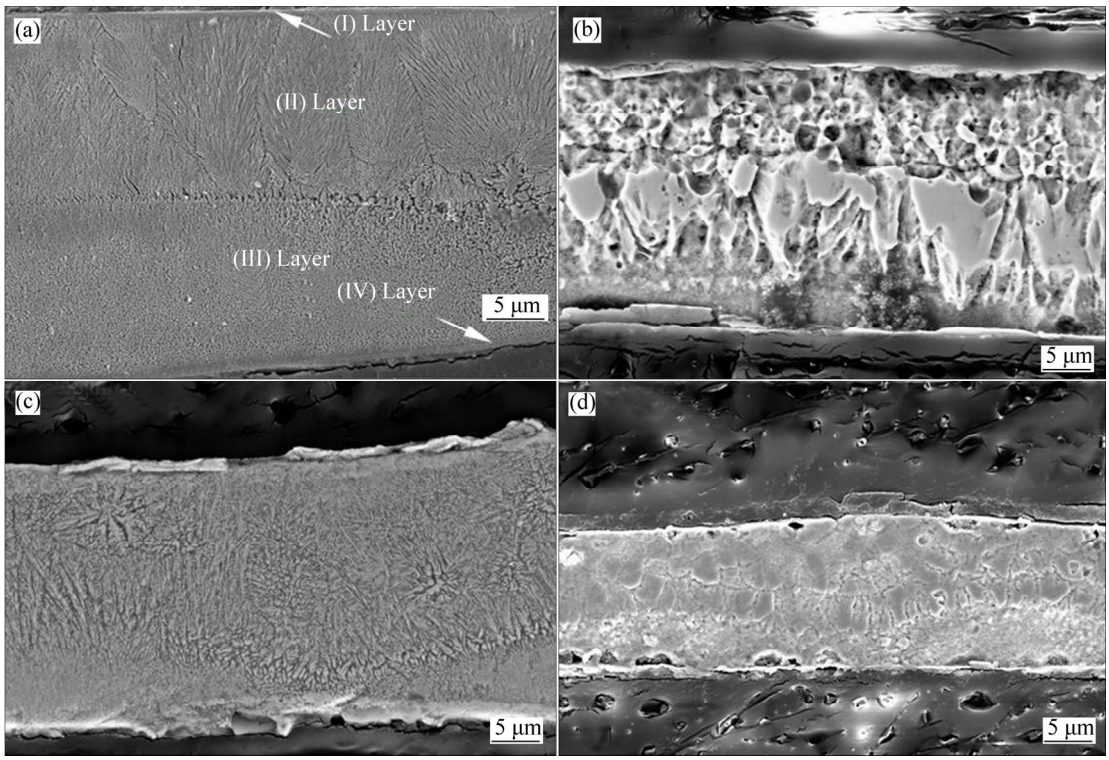

Fig. 1 Microstructures of quenched $Fe_{63}Co_{32}Gd_5$ ribbons at different wheel speeds: (a) V=15 m/s; (b) V=20 m/s; (c) V=25 m/s; (d) V=35 m/s

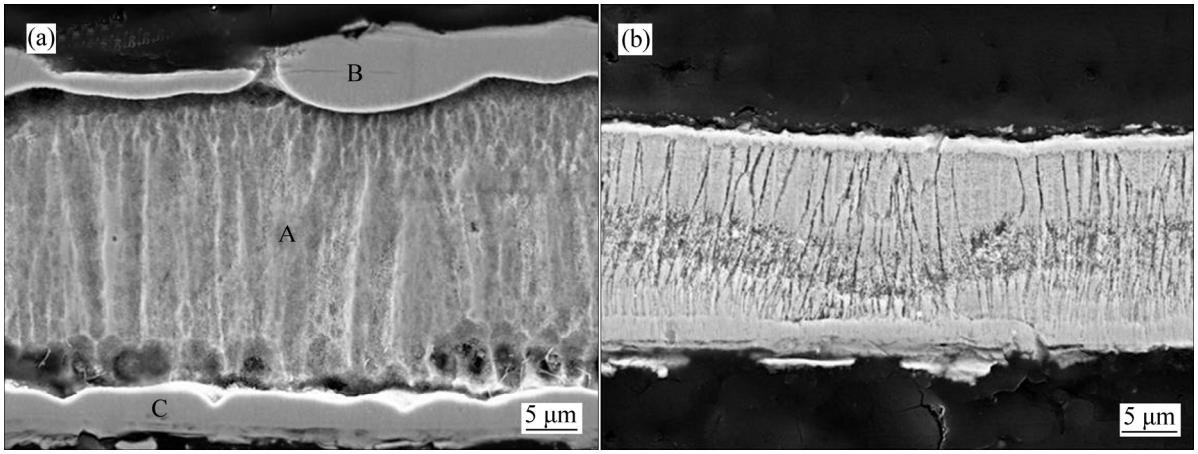

Fig. 2 Microstructures of annealed $Fe_{63}Co_{32}Gd_5$ ribbons at temperature of 823 K for 0.5 h with wheel speeds of 15 (a) and 35 m/s (b)

than that before heat treatment. The middle layer of column grain is very orderly perpendicular to ribbon plane. The layer of equiaxed grain almost disappears. In Figs. 2(a) and (b), it is clear that the thickness of surface layers of ribbon at 15 m/s wheel speed is much larger than that of ribbon at 35 m/s wheel speed. Evidently, the heat treatment benefits the growth of column grain.

In order to determine the phases of each layer, the EDS tests were carried out. Figure 3 illustrates the EDS spectra of three layers in the annealed ribbon with 15 m/s wheel speed, in which, A, B and C correspond to the middle layer, the free surface layer and the wheel surface layer, respectively. Apparently, three layers are composed of a same phase composition, although the solubilities of Gd are different. Table in each EDS spectrum presents the element content of the corresponding layer, which indicates that two surface layers have the same content, and that the middle layer has a lower solution of Gd.

When the wheel speed becomes larger from 15 to 35 m/s, the ribbon thickness is reduced, as shown in Fig. 4. When the wheel speed varies from 15 to 35 m/s, the annealed ribbon thickness reduces from 43 to 18 m. Comparing the thickness of quenched and annealed ribbons under same wheel speed, it can be clear that the heat treatment makes the ribbon thickens. When the wheel speed is 15 m/s, the ribbon is thickened by 159%, whereas the ribbon thickness varies 102% as the wheel speed is enhanced to 35 m/s. Ribbon thickening by heat treatment becomes feebler and feebler with the increase of the wheel speed. In the annealed ribbons, the layer thickness of column grain is measured, and the thickness ratio of this layer to the whole ribbon is also shown in Fig. 4. It can be seen that the thickness ratio of column grain layer to the ribbon thickness also decreases with the rise of the wheel speed.

3.2 Magnetic properties

Hysteresis loops of quenched and annealed ribbons under different wheel speeds have been measured by VSM, as shown in Fig. 5, based on which the average saturation magnetization M_s, and the coercivity H_c can be obtained. The magnetic properties derived from the Fig. 5 are listed in Table 1. In order to show directly the effect of wheel speed on the magnetic properties of quenched and annealed ribbons, the data listed in Table 1 are used in Fig. 6.

From Fig. 6, it is obvious that with the increase of wheel speed from 15 to 25 m/s, the coercivity of quenched and annealed $Fe_{63}Co_{32}Gd_5$ ribbons both have the inflection point at the wheel speed of 20 m/s, and the tendency is declined. The variation of remanence with the wheel speed is similar to that of coercivity. The saturation magnetization of quenched ribbons increases with the enhancement of wheel speed, whereas that of annealed ones decreases firstly and then increases. Therefore, at high wheel speed, the ribbons can obtain high cooling rate to form finer microstructure, which contributes to the excellent magnetic properties. Under the same wheel speed, the coercivity of annealed ribbons is lower than that of quenched ones, and the saturation magnetization of annealed ribbons are bigger than that of quenched ones. Consequently, it is clear that the heat treatment is effective to improve the magnetic properties.

3.3 Effect of grain orientation

Because the grain orientation can be reflected partly from the X-ray diffraction patterns, we performed this analysis and the results of the as-spun and the heat-treated ribbons are shown in Fig. 7. Clearly, from the XRD results of the quenched and annealed $Fe_{63}Co_{32}Gd_5$ ribbons under the wheel speeds of 15, 20, 25 and 35 m/s, there is no apparent peaks of $(Fe,Co)_{17}Gd_2$ compound in

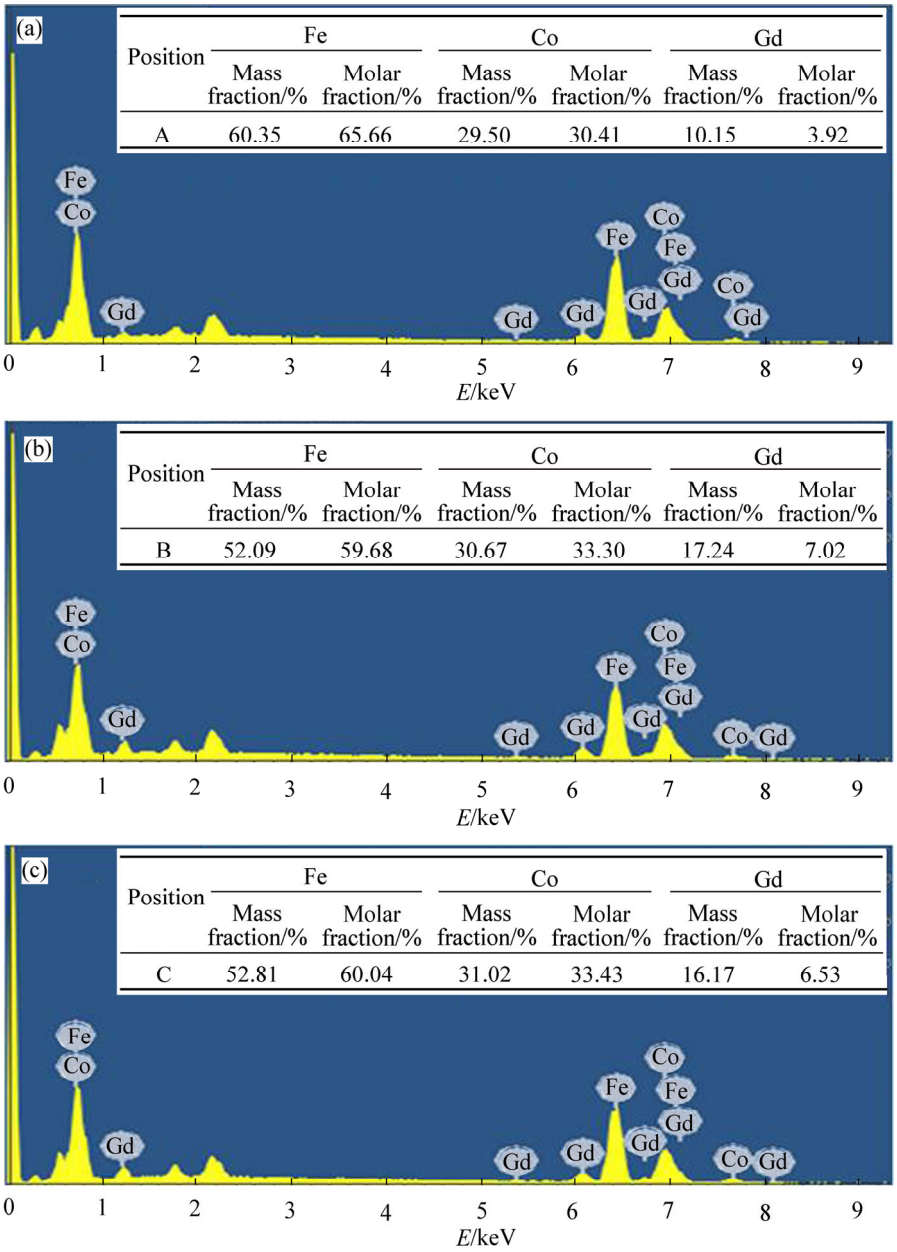

Fig. 3 EDS spectra of annealed $Fe_{63}Co_{32}Gd_5$ ribbons in wheel speed of 15 m/s: (a) Position A; (b) Position B; (c) Position C

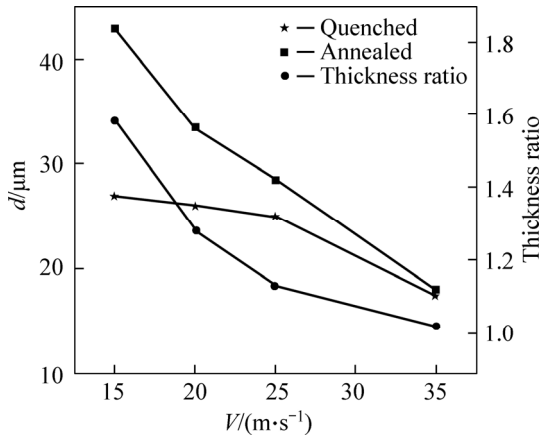

Fig. 4 Thickness of quenched and annealed $Fe_{63}Co_{32}Gd_5$ ribbons, and thickness ratio of dendritic zone versus wheel speed

the quenched ribbons. From Fig. 7(a), it can be seen that peaks (111), (200) and (211) of (Fe,Co) solid appear at each wheel velocity. Normally, the intensity of peak (111) is stronger than that of peak (200). This is a general characteristic for all the rapidly solidified ribbons. When the wheel speed increases from 15 to 35 m/s, it is found that nearly all the intensity ratios of peaks (211), (200) and (110) increase. However, the strength of peak (111) over that of peaks (200) and (211) is weakened with the increase of the wheel speed. In the higher wheel speeds of 25 and 35 m/s, the ribbons form a little $(Fe,Co)_{17}Gd_2$ compound, the peak (001) of which can be seen in Fig. 7(a). Compared with the peaks of (Fe,Co) solid, the peak (001) of $(Fe,Co)_{17}Gd_2$ compound is wider and lower. This implies that some nanocrystals of $(Fe,Co)_{17}Gd_2$

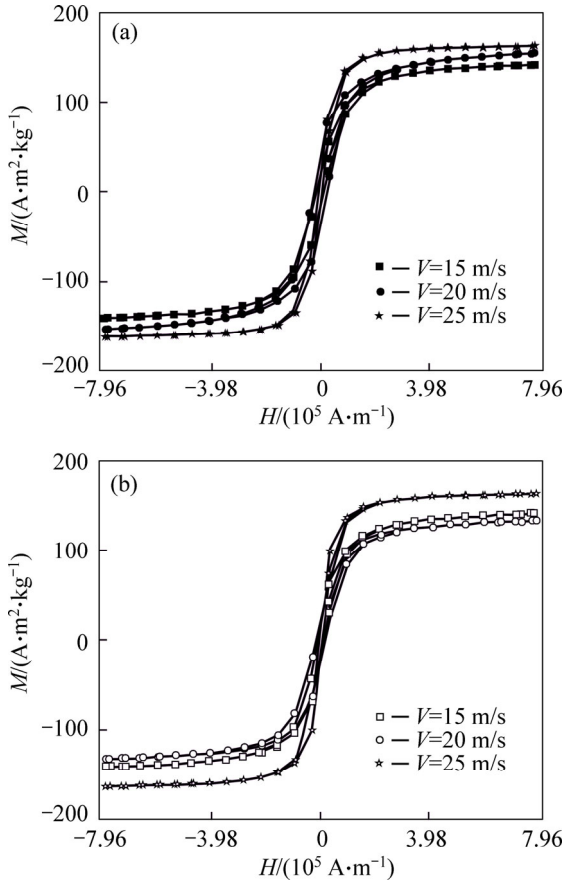

Fig. 5 Hysteresis loops of $Fe_{63}Co_{32}Gd_5$ alloy ribbons at room temperature: (a) Quenched; (b) Annealed

Table 1 Magnetic properties of quenched and annealed $Fe_{63}Co_{32}Gd_5$ ribbons at different wheel speeds

Alloy	V/ ($m·s^{-1}$)	H_c/ (10^4 $A·m^{-1}$)	M_r/ ($A·m^2·kg^{-1}$)	M_s/ ($A·m^2·kg^{-1}$)
$Fe_{63}Co_{32}Gd_5$	15	1.25	17.60	142.38
	20	2.08	35.60	155.12
	25	0.64	17.19	163.01
$Fe_{63}Co_{32}Gd_5$ (823 K)	15	1.06	19.82	141.78
	20	1.49	21.03	133.28
	25	0.53	15.17	163.62

compound exist in the ribbons. After the heat treatment, some changes takes place in the crystal structure of ribbons. Figure 7(b) shows that the heat preservation is benefitial to the formation of $(Fe,Co)_{17}Gd_2$ nanocrystals. In the thicker ribbons of 15 m/s, crystal plane (110) of $(Fe,Co)_{17}Gd_2$ compound gives a strong peak close to the peak (111) of (Fe,Co) solid solution. At the wheel speed of 20 m/s, the peak (110) of $(Fe,Co)_{17}Gd_2$ compound is higher than the peak (111) of (Fe,Co) solid solution. However, the peak of $(Fe,Co)_{17}Gd_2$ compound weakens as the wheel speed rises to 25 m/s. When the wheel speed reaches to 35 m/s, the peaks of $(Fe,Co)_{17}Gd_2$ compound almost disappear. This indicates that the heat

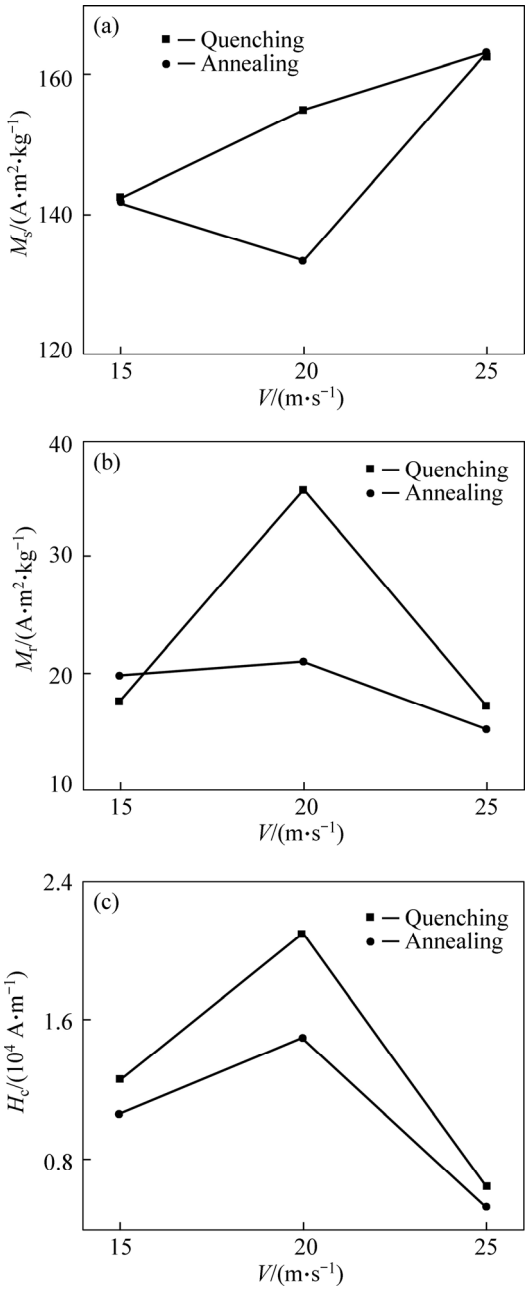

Fig. 6 Coercivity, remanence and saturation magnetization of quenched and annealed $Fe_{63}Co_{32}Gd_5$ ribbons at wheel speeds of 15, 20 and 25 m/s: (a) M_s; (b) M_r; (c) H_c

treatment makes the $(Fe,Co)_{17}Gd_2$ compound form better in ribbons of low wheel speed than in ribbons of high wheel speed.

The measured coercivity can be regarded as the average value of H_c of all grains. The better the grain orientation, the lower the coercive force [14−15]. In the present work, due to the order improvement of $(Fe,Co)_{17}Gd_2$ compound, H_c has the tendency to decrease after the heat treatment. M_s of $Fe_{63}Co_{32}Gd_5$ ribbons increases after the heat treatment process. The mechanism of this phenomenon is not clear now. More works should be performed further on this aspect.

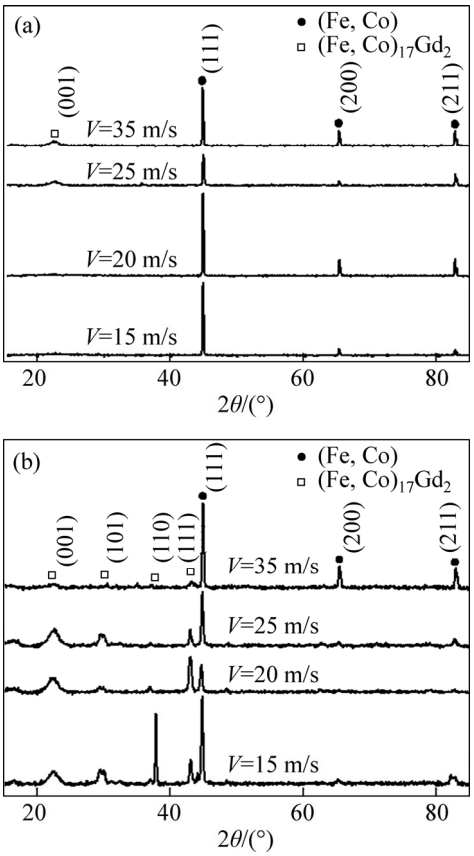

Fig. 7 XRD patterns of quenched and annealed $Fe_{63}Co_{32}Gd_5$ ribbons at wheel speeds of 15, 20, 25 and 35 m/s: (a) Quenched; (b) Annealed

4 Conclusions

By using the melt spinning technique, the $Fe_{63}Co_{32}Gd_5$ ribbons are prepared at the wheel speeds of 15, 20, 25 and 35 m/s. The rapid solidification microstructures are characterized by (Fe,Co) solid solution as the main phase with a little amount of $(Fe,Co)_{17}Gd_2$ compound in the interdendritic space. Dendrite refinement takes place with the increase of the wheel speed. After 0.5 h heat treatment at 823 K, the middle layer of column grain is very orderly perpendicular to the ribbon plane. The minimum coercivity is 5.30×10^3 A/m and the maximum saturation magnetization is 163.62 $A\cdot m^2/kg$, which is obtained in the conditions of the wheel speed 35 m/s and 0.5 h heat treatment at the temperature of 823 K.

References

[1] ZHANG C L, WANG D H, HAN Z D, XUAN H C, GU B X, DU Y W. Large magnetic entropy changes in Gd–Co amorphous ribbons [J]. Journal of Applied Physics, 2009, 105: 013912.

[2] LU S, TANG M B, XIA L. Excellent magnetocaloric effect of a Gd55Al20Co25 bulk metallic glass [J]. Physica B: Condensed Matter, 2011, 406: 3398−3401.

[3] DONG Q Y, SHEN B G, CHEN J, SHEN J, WANG F, ZHANG H W, SUN J R. Large magnetic refrigerant capacity in $Gd_{71}Fe_3Al_{26}$ and $Gd_{65}Fe_{20}Al_{15}$ amorphous alloys [J]. Journal of Applied Physics, 2009, 105: 053908.

[4] DU J, ZHENG Q, LI Y B, ZHANG Q, LI D, ZHANG Z D. Large magnetocaloric effect and enhanced magnetic refrigeration in ternary Gd-based bulk metallic glasses [J]. Journal of Applied Physics, 2008, 103: 023918.

[5] SCHWARZ B, PODMILJSAK B, MATTERN N, ECKERT J. Magnetocaloric effect in Gd-based $Gd_{60}Fe_xCo_{30-x}Al_{10}$ metallic glasses [J]. Journal of Magnetism and Magnetic Materials, 2010, 322: 2298−2303.

[6] SEHWARZ B, MATTERN N, LUO Q, ECKERT J. Magnetic properties and magnetocaloric effect of rapidly quenched Gd–Co–Fe–Al alloys [J]. Journal of Magnetism and Magnetic Materials, 2012, 324: 1581−1587.

[7] ONO H, TAYU T, WAKI N, SUGIYAMA T, SHIMADA M, KANOU M, YAMAMOTO H, TAKASUGI K, Crystallization behavior and magnetic properties of the low rare-earth content (Nd=6at.%) Nd-Fe-Co-V-B nanocomposite magnet ribbons prepared by rapid quenching method [J]. Journal of Applied Physics, 2003, 93: 8113−8115.

[8] MA SC, CAO QQ, XUAN HC, ZHANG CL, SHEN LJ, WANG DH, DU YW, Magnetic and magnetocaloric properties in melt-spun and annealed $Ni_{42.7}Mn_{40.8}Co_{5.2}Sn_{11.3}$ ribbons [J]. Journal of Alloys and Compounds, 2011, 509: 1111−1114.

[9] SUN Ji-bing, Javed A, ZHANG Zhe-xu, CUI Chun-xiang, ZHANG Miao-xin, HAN Rui-ping, Effect of B addition on the microstructure and magnetic properties of melt-spun $Sm_{12}Co_{60-x}Fe_{19}Cu_6Zr_3Bx$ ($0\leq x\leq3$) ribbons [J]. Materials Science and Engineering B, 2010, 167: 102−106.

[10] PENTON-MADRIGAL A, TURTELLI R-Sato, ESTEVEZ-RAMS E, GRÄOSSINGER R, Structural evolution with Nb content in melt-spun $Fe_{80-x}Si_{20}Nb_x$ ribbons [J]. Journal of Alloy and Compounds, 2005, 395: 63−67.

[11] RAMA RAO N V, GOPALAN R, MANIVEL RAJA M, CHANDRASEKARAN V, SURESH K G. Mössbauer studies on structural ordering and magnetic properties of melt-spun Ni–Fe–Ga ribbons [J], Applied Physics Letter, 2008, 93: 202503.

[12] SUÑOL J J, SAURINA J, BRUNA P, Structural and thermal changes induced by mechanical alloying in a Fe–Ni based amorphous melt-spun alloy [J]. Mater Chem Phys, 2009, 114: 996−999.

[13] KURZ W, FISHER D J, Fundamentals of Solidification [M]. 4th Ed, Switzerland: Trans Tech Pub Ltd, 1998.

[14] GUPTA K, RAINA K K, SINHA S K, Influence of process parameters and alloy composition on structural, magnetic and electrical characteristics of Ni–Fe permalloys [J]. Journal of Alloy and Compounds, 2007, 429: 357−364.

[15] ZOU Pei, YU Winnie, Bain J-A, Influence of stress and texture on soft magnetic properties of thin films [J]. IEEE Transactions on Magnetics, 2002, 38: 3501−3520.

(Edited by DENG Lü-xiang)